Non-Rigid Image Registration based on Form Transformations

Daniel Pimentel, María Elena Algorri, José Luis Mosso*, Gerardo Arrellín*

Instituto Tecnológico Autónomo de México, Sistemas Digitales
Río Hondo No. 1, Progreso Tizapán, 01080 D.F., México
danielpimentelalarcon@gmail.com, algorri@itam.mx
*Escuela de Medicina, Universidad Panamericana Mixcoac, México D.F.

Abstract. Image registration is an important tool for clinical diagnosis and treatment. Its objective is to find a geometrical transformation that allows the precise alignment of two different images of the same anatomical scene so that their information can be mutually enriched. The image registration method reported in this paper establishes a correspondence between regions in the images based on their form. The registration starts with a rigid alignment using affine transformations followed by a non-rigid transformation based on a thin-plate spline. We registered two MRI thoracic studies of a rabbit, and a set of MRI, PET and SPECT studies of a human brain. Experimental results were evaluated using Mutual Information as similarity criterion.

Keywords: Rigid and non-rigid image registration, thin-plate splines.

1 Introduction

Medical image registration is needed to compare or to integrate the information of different images of the same anatomical scene. The images can present variations due to changes in patient position, acquisition times, nature or calibration of the sensors (MR, PET, etc.), anatomical functioning (breathing, digestion, etc.), evolution of pathologies, or even because they were taken from different patients.

Image registration is the process of aligning two images, transforming one of them (floating image), to maximize its similarity with respect to the other (reference image), so that they can be related, compared and their information complemented.

Since registered images have a common reference frame, it becomes easier to monitor subtle changes in size or intensity in anatomical structures. Other applications of image registration are: To complement the information of multimodal images, to monitor anatomical changes through time or though medical treatment, to identify lesions, to make 3D reconstructions, for use in computer assisted surgery or even in statistical studies [5].

In fact, image registration has become an invaluable resource in biomedical research, particularly in neurosciences, where multimodal imaging has substantially contributed to the study of brain functioning [2].

Many image registration methods can be found in literature, with techniques varying, depending on the application and image type [1], from surface analysis [10,14], to evolutive computing [11,12] and neural networks [9]. The most popular methods are those based on measures of similarity [3,4,5,6], on geometrical features [7,8], and on domain transformations [13, 14, 15].

In this paper we present a non-rigid registration method based on geometrical features, particularly forms, that can register single and multimodal images with good precision. We show our results on two MRI axial studies of a rabbit's thorax (Fig. 1) as well as on a set of axial multimodal studies of a human brain. To evaluate our registration results we used the Mutual Information [16,17] of the images based on Shannon's entropy, before and after registration to measure the increase in image similarity. The results are presented in compact form using confidence intervals [20].

2 Method

The method reported in this paper uses a correspondence between the forms of regions in the images. The method transforms the forms of the regions in the floating image to adjust them to the forms of the regions in the reference image. The method consists of four stages: Preprocessing, feature extraction, preliminary rigid registration and non-rigid registration.

2.1 Preprocessing

Given the amount of noise present in the medical images that were used in the experiments, it was necessary to improve their quality before undergoing registration. Preprocessing of the images consisted of contrast enhancement, noise removal and edge detection. The algorithms used are described in [18]. The images shown in this paper have all been preprocessed.

2.2 Feature Extraction

After preprocessing, the method extracts the features that are common to the two images to be registered, so that a common coordinate frame can be established for both of them. The features used by the method are the exterior contour of the patient, the anatomical center and the main direction of the images (Fig. 1).

Exterior contour. To find the exterior contour of the images, these are first binarized to identify the coordinates of the foreground pixels with value $I(x,y)=1$. From these pixels we obtain the convex hull [32] using Graham's scanning algorithm [31]. The convex hull can present discontinuities, so it was necessary to complete the information of the contour represented by the convex hull using interpolation. We tried two different interpolation methods:

Splines: All the pixels of the convex hull were interpolated with a natural spline [33].

Nearest Neighbors: Although the convex hull is a closed form, sometimes consecutive pixels over it lie far away from each other in pixel space. This is the case of pixels over the convex hull that border concave sections of the contour, since such concave sections are far away from the convex hull. To better define the contour over such sections we drew an imaginary line over the distant (but consecutive) pixels of the convex hull and looked for the pixels of the binary image whose perpendicular distance to the imaginary line was shortest. Just a few additional pixels need to be found in this way, since then a new spline interpolation can be conducted over the pixels to complete the contour information.

Both methods are used distinctively depending on the concavity of each section of the contour: if the section is convex, interpolation with splines is used, if the section is concave we used a nearest neighbor search.

Anatomical center. Once the exterior contour is found, the anatomical center is calculated as the weighted average (*ex, ey*) of the coordinates of the contour.

Principal direction. By finding the principal direction of the reference and floating images, a common orientation can be calculated for them. Depending on the images, the methods to find the principal direction can vary considerably, from determining the longest axis of the image contours, to looking for specific patterns in the represented anatomy. Finding a common orientation for two very different images can be prone to errors, and in the worst case, when the direction cannot be determined automatically, the images can be annotated, or the principal direction determined interactively by a variety of methods [9], until the optimal direction is found when the Mutual Information of the registered images is maximized.

In our method, the longest axis of the contour was used as the principal direction of the reference images. However, due to the circularity of the floating images and to their high noise content, it was necessary to annotate them manually by clicking on the position of the rabbit's vertebrae in every image. The principal direction was then established as the vector passing through the anatomical center of the images and through the position of the vertebrae.

2.3 Preliminary Rigid Registration

Rigid registration is a necessary step to align the images based on their anatomical center and principal direction. Rigid registration gives both images a common anatomical center and a common principal direction as seen in Fig. 1, and it avoids unnecessary processing during non-rigid registration [1]. Rigid registration is carried out using a translation and a rotation matrix [21].

2.4 Non-rigid Registration

For the non-rigid registration, a correspondence relationship has to be established between the points that form the contour of the reference image F_R, and the points that form the contour of the floating image F_F. There are various ways of establishing a correspondence between the points of the two contours. A simple one consists of associating every point along the reference contour with another point along the floating contour following a given criteria. We use this approach as follows: Let p_i be a point of F_R and e the common anatomical center of both images after rigid registration. Let l_i be the line that passes through e and p_i with equation: $y = m_l x + b_l$.

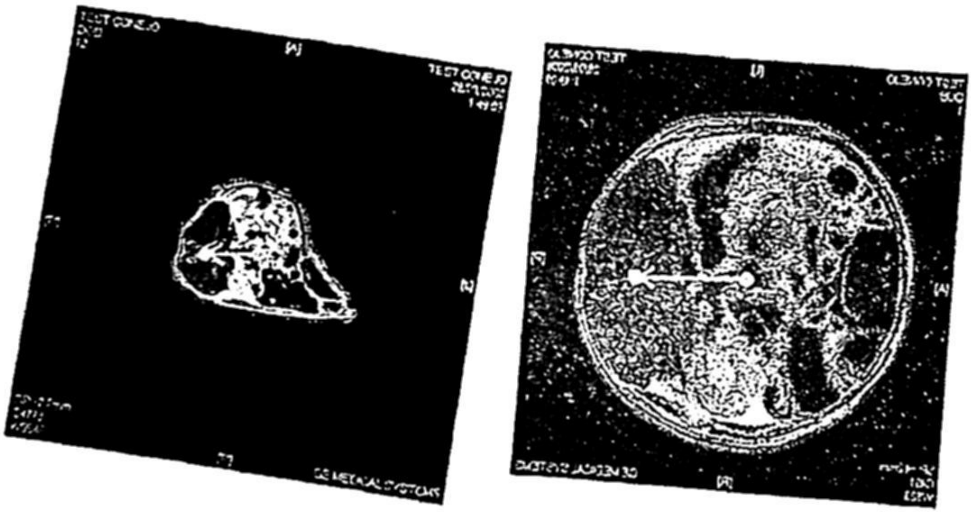

a) b)

Fig. 1. (a) Reference image after rigid alignment. (b) Floating image after rigid alignment.

To determine the exact point q_i on F_F that corresponds to p_i we look for the intersection of l_i and F_F (Fig. 3). We find the exact intersection point p_i using a line-line intersection strategy. The first line is l_i and the second line is the line formed by two consecutive points (x_i, y_i) (x_{i+1}, y_{i+1}) over F_F that intersects l_i at a point (x,y) lying along the path between (x_i, y_i) and (x_{i+1}, y_{i+1}). Since we are dealing with discrete images, it is possible that q_i does not exactly belong to the finite set of points in F_F, in which case an interpolation is necessary.

Thin-plate-spline Deformation. Thin-plate splines [22] are bivariate interpolation functions based on physical principles that can be used to interpolate an arbitrary set of coordinates *(x,y,f(x,y))*. These splines are a generalization of the natural cubic spline for one dimension. They represent the minimal deformation that allows the coordinates of a metal sheet (x_i, y_i) to adjust themselves to the new set of coordinate values (x_i', y_i') that is specified by the correspondence of contours. The idea is to model the floating image as a metal sheet, and make the contour points in it adjust themselves exactly to their corresponding points on the contour of the reference image. The rest of the pixel values $f(x_i, y_i)$ in the floating image are interpolated to adjust them to the new coordinate values specified by the correspondence. We must then find the function f(x,y) that minimizes:

$$\iint \left(\frac{\partial^2 f}{\partial x^2}\right)^2 + \left(\frac{\partial^2 f}{\partial x y}\right)^2 + \left(\frac{\partial^2 f}{\partial y^2}\right)^2 dxdy \ , \tag{1}$$

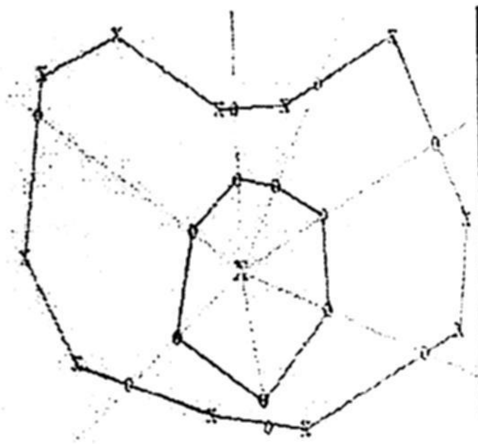

Fig. 2. (a) Method used to determine the correspondence of points in both contours. The anatomical center is represented by the middle X. The circles along the inner contour are the points that form the reference contour, the X's on the exterior contour are the points that form the floating contour. To find the points over the floating contour that correspond to the points on the reference contour, a ray-line is traced from the common center that passes through each point in the reference contour and intersects the floating contour. The exact intersection point is found using a line-line intersection algorithm. The circle points along both contours are then associated and will determine the deformation that the floating image will undergo. b) The correspondence method between both contours is illustrated in two MR images of the rabbit.

commonly known as the energy deformation function of the thin-plate spline. This function is minimized through the solution of a system of linear equations:

$$f(x,y) = a_0 + a_x x + a_y y + \sum_{i=1}^{n} \omega_i U(|x - x_i, y - y_i|) \ , \tag{2}$$

where:

$$U(t) = r^2 \log(r) \tag{3}$$

is the well known fundamental solution to the bi-harmonic equation $\Delta^2 U = 0$, that satisfies the condition of minimum energy deformation, $|\cdot|$ indicates the length of a vector, and the coefficients a_0, a_x, a_y, and ω_i are determined by the requirements of an exact interpolation, such that by the proper choice of ω_i, $f(x,y)$ maps the intensities of the pixels in the floating image from their original coordinate space to the coordinate space specified by the correspondence of both images. Thin-plate splines provide a soft interpolation for derivatives of any order, they do not require manual specification of parameters, they offer a closed solution and a physical explanation of their energy function. By applying the thin-plate spline deformation to the floating image, we assign the intensity values of the pixels on its exterior contour, to the corresponding pixels on the exterior contour of the reference image, carrying out a bivariate interpolation of all the other pixel values on the floating image and applying them to their new positions on the reference image, to obtain the desired registered image as shown in Fig. 3.

3 Experimental Results

We acquired two MR studies, each of 20 images of the thoracic region of a rabbit. The first study was taken with the rabbit placed free in the scanner and using the full magnet that is used to take studies of adult patients. The second study was taken with the rabbit inside a smaller magnet usually used to take images of a hand or foot. The images had a resolution of 512 x 512 and a spatial separation of less than a centimeter. The images of the first study were established as reference images (Fig. 1a), and the images of the second study were the floating images (Fig.1b).

In an attempt to obtain a quantitative evaluation of the registration results, we used Mutual Information as a similarity measure of the registered images [23-30]. Statistically, Mutual Information can be interpreted as the dependency measure between two sub experiments X and Y, having two sampling subspaces S_x and S_y.

$$\left.\begin{array}{l} S_X = \{x_1, x_2, x_3, \ldots, x_m\} \\ S_Y = \{y_1, y_2, y_3, \ldots, y_n\} \end{array}\right|, \tag{4}$$

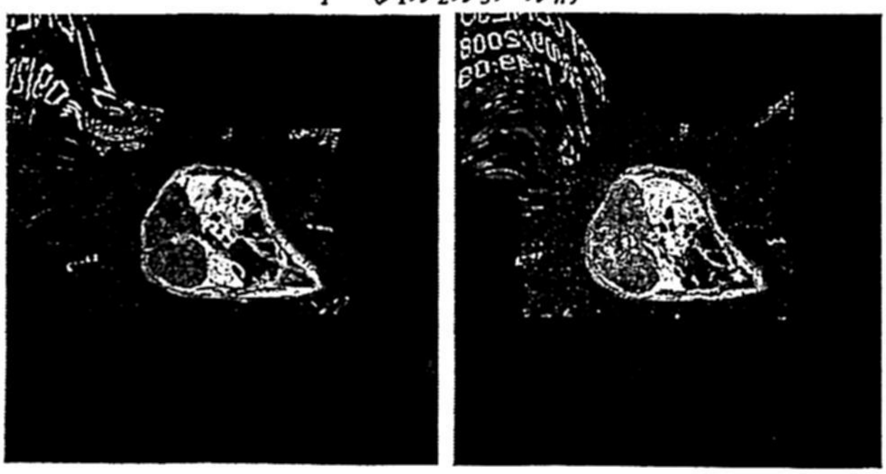

Fig. 3. Registered images.

With $p(x_i)$ and $p(y_i)$ the probabilities of events x_i and y_i respectively. To evaluate the similarity between the reference and the floating images, we consider the reference image, sub experiment X, and the floating image, sub experiment Y, and we define the sampling subspaces as the possible intensity values of the pixels in the images. Mutual information is defined as:

$$\begin{aligned} I(X;Y) &= H(Y) - H(Y \mid X) \\ &= H(X) + H(Y) - H(X,Y) \\ &= \sum_{i=1}^{m}\sum_{j=1}^{n} p(x_i, y_j)\log\left(\frac{p(x_i, y_j)}{p(x_i)p(y_j)}\right) \end{aligned}, \qquad (5)$$

where $H(Y)$ is Shannon's entropy[17] of Y, $H(Y|X)$ is the entropy of Y given X, and $H(X,Y)$ is the joint entropy of X and Y.

When the images have minimum similarity, that is, when they are independent events, the mutual information between I_R and I_F (reference and floating images) is minimal, and when the images are completely dependent from each other, their mutual information is maximal.

We present here the results of measuring the mutual information between pairs of images in terms of 95% confidence intervals using the t-Student distribution [20] for three cases: OMI (original mutual information of the images before registration) as $I(I_R;I_F)$, RMI (mutual information after registration) as $I(I_R;I_R)$, and MMI (maximal mutual information $H(I_R)$). Note that MMI implies that both images are the same, meaning they have no complimentary information, which is a non-desired outcome and is shown here just for comparison. The results obtained are shown in Table 1 where it can be seen that, for 95 out a 100 registered images, their mutual information increased from 0.0406 to 0.2519, and from 0.0546 to 0.2893, that is a 5-fold increase.

Tabla 1. 95% Confidence Intervals

Measurement	Confidence Interval
$I(I_R,I_F)$	$P(0.0406 \le OMI \le 0.0546) = 0.95$
$I(I_R,I_T)$	$P(0.2519 \le RMI \le 0.2893) = 0.95$
$H(I_R)$	$P(0.9628 \le MMI \le 1.1370) = 0.95$

Although the conventional notation is to express confidence intervals in terms of probabilities, the correct interpretation is that if an experiment were realized once and again, in 95% of times, the value of mutual information would be between the limits of the confidence interval for each case.

4 Analysis

Most image registration methods propose iterative searches throughout the method to obtain the best registration parameters. In the method used in this paper, the parameters to use are only those of the preprocessing stage plus the principal direction of the images. The required preprocessing parameters are the size of the averaging filters, the degree of membership in the fuzzy logic algorithms, the noise removal and binarization threshold values. The direction of the images can vary from 0° to 360°, and, if impossible to determine automatically, it can be found through an iterated search where the direction angle is varied in the floating image, until the best registration is achieved.

The variability of the parameters to achieve the best possible registration depends largely on the amount of noise present in the images. Proof of this are the reference images which are almost noise free and where the parameters were never changed, and even if they were slightly modified, the results showed almost no variation. On the other hand, for some of the very noisy floating images only a small set of parameter values resulted in adequate registrations. These successful parameter values were determined iteratively looking for registration results that provided the largest increase in mutual information. Noise also makes the process of determining the direction of the images, prone to error. And even the process of iteratively looking for parameter values can be contaminated, especially since the mutual information criterion is not infallible.

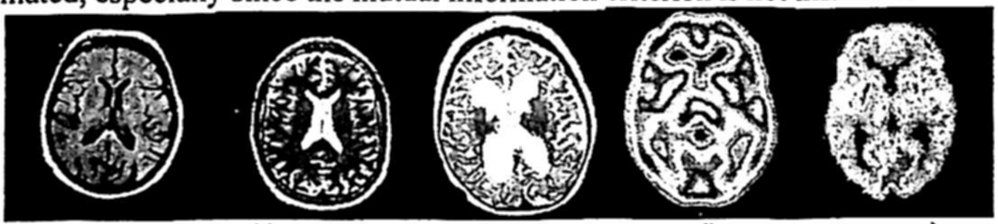

a) b) c) d) e)

Fig. 4. (a) MR reference image, (b-e) MR, MR, PET, SPECT floating images

We wanted to further test the flexibility of the reported method and its applicability to other types of medical images, so we did an experiment on brain axial images. We downloaded 5 multimodal brain studies (Fig.4): three MRIs, one SPECT and a PET. The results of this image registration experiment are shown in Fig. 5.

Fig. 5. Registered images.

5 Conclusions

Experimental results show that the non-rigid registration method reported in this paper can achieve high precision results while maintaining flexibility of application. As in all image-processing tasks, noise is a big issue. The success of the image registration method largely depends on the success with which noise is removed from the images. Noise is the main cause for parameters being manually or iteratively adjusted. Besides noise, determining the principal direction of the images was the biggest challenge, and if some a-priori information can be used to precisely determine it without manual intervention, then the method becomes a good candidate for real time unsupervised registration.

Mutual information is a measure of similarity that, while not infallible, offers a solid similarity measure that allows the user to choose the best registration results especially when parameters must be determined iteratively.

Many areas in image processing can complement the results of image registration. Some examples are automatic image segmentation and classification, whose results can then lead to very precise registrations [1]. Our future work is focused on adding more specialized image processing tasks to the registration pipeline to increase its precision, flexibility and applicability.

References

1. Gottesfeld B. L., "A survey of image registration techniques", ACM Computing Surveys Vol. 24, Num. 4, 1992, pp. 325-376.
2. Joseph V. Hajnal, Derek L.G. Hill, David J. Hawkes, Medical Image Registration, CRC Press LLC, 2001.
3. R. Oeuvray and M. Bierlaire, "A new derivative-free algorithm for the medical image registration problem", International Journal of Modelling and Simulation, Vol. 27, Num. 2, 2007, pp. 115-124.
4. Shaoyan Sun, Liwei Zhang, and Chonghui Guo, "Medical Image Registration by Minimizing Divergence Measure Based on Tsallis Entropy", International Journal of Biomedical Sciences, Vol. 2, Num. 2, 2007, pp. 75-80.
5. Xiu Ying Wang, David Dagan Feng, Jesse Jin, "Elastic Medical Image Registration Based on Image Intensity", Int. Journal of Imag. and Graphics, Vol. 5, Num. 2, 2005, pp. 351-369.
6. S. Korukonda, MC. Prakash, R. Venkatachalam, and S. Ramasway, "Information theory based image registration", Review of Quantitative Nondes-tructive Evaluation, Vol. 26, 2007, pp. 531-538.
7. Hai-Ping Ren, Hu Yang, Bing-Rong Ma, Sheng-Zu Chen, andWen-KaiWu, "A novel magnetic resonance-positive emission image registration based on morphology", Bio-Medical Materials and Engineering, Vol. 13, 2003, pp. 187-196.
8. Jianhua Xuan, Yue Wang, Matthew T. Freedman, Tulay Adali, and Peter Shields, "Nonrigid Medical Image Registration by Finite-Element Deformable Sheet-Curve Models", International Journal of Biomedical Imaging, Vol. 2006, 2006, pp. 1-9.
9. Lifeng Shang, Jian Cheng Lv, Zhang Yi, "Rigid medical image registration using PCA neural network", Neurocomputing Vol. 69, 2006, pp. 1717-1722.
10. Berthold K. P. Horn et. al, "Using Synthetic Images to Register Real Images with Surface Models", Communications of the ACM, Vol. 21, Num. 11, 1978, pp. 914-924.
11. Flávio Luis Seixas, Luiz Satoru Ochi, Aura Conci, Débora C. M. Saade, "Image Registration Using Genetic Algorithms", GECCOí08 ACM, Julio 2008, pp. 1145-1146.
12. Ju Han and Bir Bhanu, "Hierarchical Multi-sensor Image Registration Using Evolutionary Computation", GECCO í05 ACM, 2005, pp. 2045-2052.

13. Tarek A. El-Ghazawi, Prachya Chalermwat, Jacqueline Le Moigne, "Wavelet-Based Image Registration on Parallel Computers", ACM, 1997.
14. Q. P. Zhang, M. Liang, and W.C. Sun, "Multi-resolution image data fusion using 2-D discrete wavelet transform and self-organizing neural networks", ACM, 2004, pp. 297-301.
15. M. H. Malik, S. A. M. Gilani, and Anwaar-ul-Haq, ìAdaptive Image Fusion Scheme Based on Contourlet Transform and Machine Learningî, International Review on Computers and Sortware (I.RE.CO.S), Vol. 3, Num. 1, 2008, pp. 62-69.
16. Jan C A van der Lubbe, Information Theory, Cambridge University Press, 1997.
17. Roberto Togneri, Christopher J.S. deSilva, Fundamentals of Information theory and coding design, CRC Press LLC, Nueva York, 2000.
18. K. J. Ray Liu, Pattern Recognition and Image Preprocessing, 2a Edici6n, Board, 2002.
19. Rafael C. Gonzalez, Richard E. Woods, Dig. Image Processing, Pearson PH, 3rd. Ed., 2008.
20. Devore, J, Probability and Statistics for Engineering and the Sciences, 3rd Ed, Wadsworth Publishing Company, Califoria, 1982.
21. Stanley I. Grossman, Álgebra lineal, McGraw-Hill, México, 1999.
22. Bookstein, Fred L., "Principal Warps: Thin-Plate Splines and the Descomposition of Deformations", IEEE Transactions on Pattern Analysis and Machine Intelligence, Vol. 11, No. 6, 1989, pp. 567-585.
23. Amira Serifovic-Trbalic, Damir Demirovic, Naser Prljaca, and Zekerijah Sabanovic, "Evaluation of Interpolation Methods in Mutual Information-Based Medical Image Registration", Original Paper, Vol. 15, Num. 4, 2007, pp. 191-196.
24. Jiangang Liu and Jie Tian, "Registration of Brain MRI/PET Images Based on Adaptive Combination of Intensity and Gradient Field Mutual Information", International Journal of Biomedical Imaging, Volume 2007, 2007, pp. 1-10.
25. C. Fookes, M. Bennamoun, "Rigid Medical Image Registration and its Association with Mutual Information", International Journal of Pattern Recognition and Arti.cial Intelligence, Vol. 17, Num. 7, 2003, pp. 1167-1206.
26. Edward J. R. Somer, Paul K. Marsden, Nigel A. Benatar, Joanne Goodey, Michael J. O.Doherty, Michael A. Smith, "PET-MR image fusion in soft tissue sarcoma: accuracy, reliability and practicality of interactive point-based and automated Mutual Information techniques", Europ. Journal of Nuclear Med. and Molecular Imag., Vol. 30, Num. 1, 2003.
27. Philippe Thévenaz, Michel Bierlaire, Michael Unser, .Halton Sampling for Image Registration Based on Mutual Information., Sampling Theory in Signal and Image Processing, Vol. 7, No. 2, 2008, pp. 141-171.
28. Charlse R. Meyer, Bradford A. Mo□at, Kyle K. Kuszpit, Peyton L. Bland, Paul E. Mckeever, Timothy D. Johnson, Thomas L. Chenevert, Alnawaz Rehemtulla, and Brian D. Ross, "A Methodology for Registration of a Histological Slide and In Vivo MRI Volume Based on Optimizing Mutual Information", Mol. Imaging, Vol. 5, Num. 1, 2006, pp. 16-23.
29. L. Thurfjell, Y. H. Lau, J. L. R. Andersson, B. F. Hutton, "Improved efficiency for MRI-SPET registration based on Mutual Information", European Journal of Nuclear Medicine, Vol. 27, Num. 7, 2000, pp. 846-856.
30. N. Cvejic, C. N. Canagarajah, and D. R. Bull, Image fusion metric based on Mutual Information and Tsallis entropy., Electronics Letters, Vol. 42, Num. 11, 2006.
31. Graham, R. L., "An efficient algorithm for determining the convex hull of a planar set" Inform. Prec. Letlers 1, 1972, 132-133.
32. Bradley Efron, "The convex hull of a rand. set of points", Biometrika, 1965, pp. 331-343.
33. Hsieh Hou, Andrews, H., "Cubic splines for image interpolation and digital filtering", Acoustics, Speech and Signal Processing, IEEE Transactions, Vol. 26, 1978, pp. 508-517.